HYDROGEN-AIR DEFLAGRATIONS IN OPEN ATMOSPHERE: LARGE EDDY SIMULATION ANALYSIS OF EXPERIMENTAL DATA

Molkov, V.V. [1], Makarov, D.V. [1] and Schneider, H. [2]

[1] FireSERT Institute, University of Ulster, Newtownabbey, Co. Antrim, BT37 0QB, UK
[2] Fraunhofer Institut Chemische Technologie, Joseph-von-Fraunhoferstr. 7, 76327 Pfinztal, GERMANY

ABSTRACT

The largest known experiment on hydrogen-air deflagration in open atmosphere has been analysed by means of the large eddy simulation (LES) technique. The LES model of premixed combustion developed at the University of Ulster was applied to investigate the underlying physics of the phenomenon. The LES combustion model is based on the progress variable equation to simulate the propagation of the premixed flame front. The gradient method is applied for a source term in the progress variable equation to decouple the physically grounded turbulent burning velocity from a numerical grid. The transition from laminar to turbulent combustion has been considered through two main physical phenomena, i.e. hydrodynamic flame front instability and turbulence generated by the turbulent flame front itself. The hydrodynamic instability of the premixed flame front has been partially resolved by LES and its SGS effect has been modelled by the Yakhot's model of premixed turbulent combustion. Contrary to the hydrodynamic instability the turbulence generated by flame front itself takes place at SGS level only. It has been modelled based on the maximum value for flame front self-induced turbulence predicted by Karlovits *et al*. in 1951 and the transitional distance determined by Gostintsev *et al*. The chemistry and effects of the selective diffusion at scales of real flamelets are taken into account through the value of laminar burning velocity 1.91 m/s for stoichiometric hydrogen-air mixture. The LES model has been successfully validated against experimental data on the dynamics of flame propagation from the ignition source to the radius of 20 m, flame shape, positive and negative phases of the pressure wave generated by the explosion at distances up to 80 m. The model is built from the first principles and no adjustable parameters have been applied to get very good agreement with the experiment.

NOMENCLATURE

CFL	Courant-Friedrichs-Lewy number
c	Progress variable (normalised product mass fraction)
E_i	Expansion coefficient, $E_i = \rho_u / \rho_b$
g	Vector of gravity acceleration, m·s^{-2}
M	Molecular mass, kg·kmole^{-1}, $M = \sum_m V_m M_m$
p	Pressure, Pa
R	Radius, m
R_0	Radius of polyethylene hemisphere filled with hydrogen-air mixture, m
R^*	Radius for onset self-turbulised flame propagation regime, m
Re	Reynolds number, $\mathrm{Re} = S_u R_{ff} \rho_u / \mu_u$
S_c	Source term in conservation equation for progress variable, kg·m^{-3}·s^{-1}
Sc	Schmidt number
S_{u0}	Burning velocity at initial conditions, m·s^{-1}
S_u	Burning velocity, m·s^{-1}
T	Temperature, K
t	Time, s

$u_{i,j,k}$ Velocity components, m·s^{-1}

u' Root-mean square of sub-grid scale velocity component, m·s^{-1}

$x_{i,j,k}$ Spatial coordinates, m

Y_a Mass fraction of air

Greek

Δ_{CV} Control volume characteristic size, m

Δt Time step, s

μ Dynamic viscosity, Pa·s

ρ Density, kg·m^{-3}, $\rho = (pM)/(R_\mu T)$

Ξ Flame front wrinkling factor

Subscripts

b Burned mixture

cell Cellular structure

eff Effective value

i,j,k Spatial coordinate indexes

t Turbulent

u Unburned mixture

0 Initial conditions

Bars

$\bar{}$ LES filtered quantity

$\sim$ LES mass-weighted filtered quantity

1.0 INTRODUCTION

One of likely accidental scenarios is a deflagration of hydrogen-air mixture in open atmosphere at large scales. Understanding of the underlying physical phenomena is essential to develop reliable predictive tools for risk assessment and hydrogen safety engineering. Relatively high flame propagation velocity makes hydrogen-air explosions potentially more dangerous compared to the most of hydrocarbons. The theory suggests that various instabilities can strongly affect flame front propagation velocity [1].

Accidental combustion of initially quiescent premixture commences usually from a laminar flame propagation, then a flame cracking and cells formation, a cellular flame propagation, and finally a self-turbulising flame propagation [2]. The onset of the cellular structure for propane-air deflagration occurs at the flame Reynolds number about Re=10^4 [3]. If the same critical value is accepted for stoichiometric hydrogen-air flame at normal conditions (μ_u=2.3·10^{-5} Pa·s, ρ_u=0.88 kg·m^{-3}, S_u=1.91 m/s) then the flame front becomes cellular (non-laminar) already at size of 0.14 m.

The study performed by Karlovits *et al*. [4] using burner flames led to the conclusion that a flame front itself generates turbulence. The maximum theoretical value of the flame front wrinkling due to flame induced turbulence was found to be:

$$\Xi_{\max} = \frac{E_i - 1}{\sqrt{3}}, \tag{1}$$

where E_i – combustion products expansion coefficient.

Gostintsev *et al*. analysed about 20 experiments on large-scale unconfined deflagrations and came to a conclusion that the hydrodynamic flame instability leads to accelerating, self-similar regime of fully

developed turbulent flame propagation [5]. According to this analysis, the flame front surface obeys the fractal theory after self-similar regime is established. The authors found that the transition to the self-similar turbulent regime of flame propagation occurs after the critical value of the flame front radius R^* is achieved, which was found to be R^*=1.0-1.2 m for near stoichiometric premixed hydrogen-air flames. This result suggests that the characteristic features of the large-scale hydrogen-air deflagrations may be quite different from those obtained in small-scale experiments. This is in line with a recent critical review [6], where a conclusion is made that "large scale research has shown that explosions may be more severe than was previously recognised". Accordingly, there is a need to demonstrate that the models and tools used for risk assessment and hydrogen safety engineering are valid at scales typical for hydrogen applications.

2.0 OVERVIEW OF EXPERIMENTALAL DATA

The series of experiments on hydrogen-air explosions in open atmosphere was conducted in 1983 in Germany [7]. The general objective was a study of the dependence of a flame propagation velocity on a flammable mixture size. Near stoichiometric hydrogen-air mixtures were prepared in hemispherical ground-based polyethylene balloons with radius R=1.53, 2.88, 5.0 and 10.0 m. The balloon envelope was made of several PE segments, comparable to the surface of individual orange slices, which were welded together (see Figure 1). Ignition was initiated by exploding wire with energy between 10 and 1000 J or by pyrotechnical charges. The ignition device for the exploding wire contained a condenser battery with a capacitance of 320 μF, which can be loaded by a high voltage device operating between 250 V and 2500 V, so that the available energy is adjustable between 10 and 1000 J. It was found that flame propagation velocity was independent upon ignition energy in the investigated energy range. There was no dependence of turbulence factor, i.e. the ratio of maximum flame propagation velocity to initial flame propagation velocity, on ignition energy: from tests GHT 20-26 with 3.06-m diameter hemisphere turbulence factor was found to be 2.55$\pm$0.10 and 2.71$\pm$0.15 for ignition energies of 10 and 1000 J, respectively. The experimental data included the dependence of the flame front radius with time, flame front contours and pressure records at different locations up to 80 m from the ignition source.

The resulting flames propagated in almost hemispherical form with a developed flame front structure. The balloon shell stretched slightly outwards until it ruptered nearly simultaneously along the PE segments when the flame reached about half of the original radius of the balloon $0.5R_0$. The maximum visible flame velocity occurs approximately between the original radius of the balloon R_0 and radius $1.5R_0$. The maximum flame radius reached approximately $2R_0$. The observation of the flame front was made difficult when the flame front reached the expanding segments of the ruptured balloon. However, the error in the determined flame velocity was estimated as ±5%. The maximum flame propagation velocity was found to increase with the radius of the initial hydrogen-air mixture, which is quite in agreement with theoretical predictions. No transition to detonation was observed. The maximum visible flame velocity reached 43 m/s for hemisphere with initial radius R_0=1.53 m, 54 m/s for hemisphere with radius R_0=2.88 m, 60 m/s for R_0=5.0 m and 84 m/s for R_0=10.0 m. In each particular experiment the maximum peak pressure, associated with the corresponding maximum flame propagation velocity, was nearly constant for pressure sensors installed inside the hydrogen-air mixture. At a sufficient distance from the explosion the maximum pressure decayed inversely proportional to the distance. The positive pressure wave was followed by a negative pressure phase. Usually the negative pressure wave was somewhat shorter than the positive one providing larger negative pressure peak.

The largest experiment GHT 34 in the series with a radius of hemispherical 29.7% hydrogen-air mixture R_0=10 m (see Figure 1) was used to analyse the physics of the phenomenon of hydrogen-air deflagration in open atmosphere and to validate the LES model in the present study. In 2094-m^3 hemisphere experiment a rhombus-shaped wire net was laid over the hemispherical balloon which was fastened to the ground at 16 points to compensate buoyancy force. Gases inside the balloon were mixed by fans to avoid hydrogen stratification. In order to make hydrogen-air flame visible in a daylight finely ground NaCl powder was dispersed inside the balloon at the end of filling process to

produce yellow-coloured flame. Generally 10 to 12 piezo-resistive Kistler pressure sensors having 1 bar range and natural frequency 14 kHz were used. They were mounted in a steel case having a mass of 20 kg in a way that their pressure-sensitive surfaces were fitted flush with the surface of the ground and covered with 2 mm thick layer of silicone grease on the membrane to protect from influence of temperature and heat radiation. One sensor at a distance of R=5m was protected on a trial basis by means of a laminated plastic plate screwed to the steel casing and having in the middle an opening of 4-mm diameter. Besides of this specially protected sensor the pressure signal of all the other sensors being within the range of the combustion products do not return to zero after the negative pressure phase. This can be attributed to the fact that at high temperatures as present in the flame area the sensors indicate too low pressures. Obviously the additional protection of the R=5m sensor is sufficient to prevent the sensor from being influenced by high temperature combustion products, whereas silicon grease alone is not. On the other hand the pressure measurement seems not to be distorted by the additional shielding.

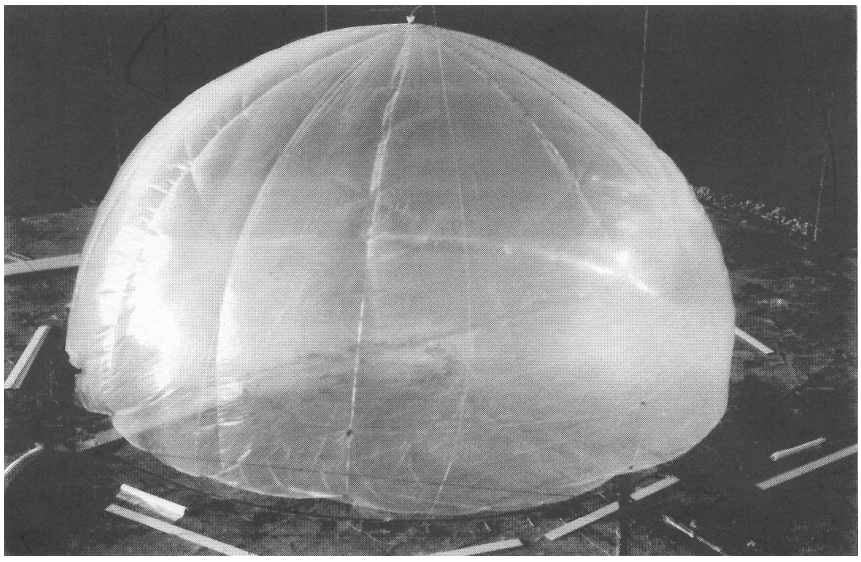

Figure 1. The hemispherical balloon with hydrogen-air mixture, R_0=10 m

There is a sharp pressure peak superimposed on the pressure time history of all the sensors installed inside the balloon. This peak occurs at the moment when the flame passes the sensor on the ground. The cause for the occurrence of this peak is not clear, but it seems to be the result of some mechanical impact associated probably with the mounting of the PE foil in the sensor housing. The energy of the ignition source was 150 J. An initial value of laminar burning velocity was estimated from the experimental data as S_u=2.39 m/s (combustion products expansion coefficient estimated by authors of experiment was 7.26 with density 0.8775 kg/m^3 and speed of sound 397.3 m/s) [7]. Video-records show the developed turbulent flame front structure at later stages of the explosion (see Figure 2). It is seen that a thickness of the turbulent flame is of the order of meters.

3.0 LARGE EDDY SIMULATION MODEL

The LES model developed at the University of Ulster and described elsewhere, e.g. [8,9], was applied to simulate the flame front propagation in the considered experiment. The model comprises filtered three-dimensional mass, momentum and energy conservation equations in fully compressible form [8]. The flame front propagation is modelled using the progress variable equation:

$$\frac{\partial}{\partial t}\left(\overline{\rho}\widetilde{c}\right)+\frac{\partial}{\partial x_j}\left(\overline{\rho}\widetilde{u}_j\widetilde{c}\right)=\frac{\partial}{\partial x_j}\left(\frac{\mu_{eff}}{Sc_{eff}}\frac{\partial\widetilde{c}}{\partial x_j}\right)+\overline{S}_c\,. \tag{2}$$

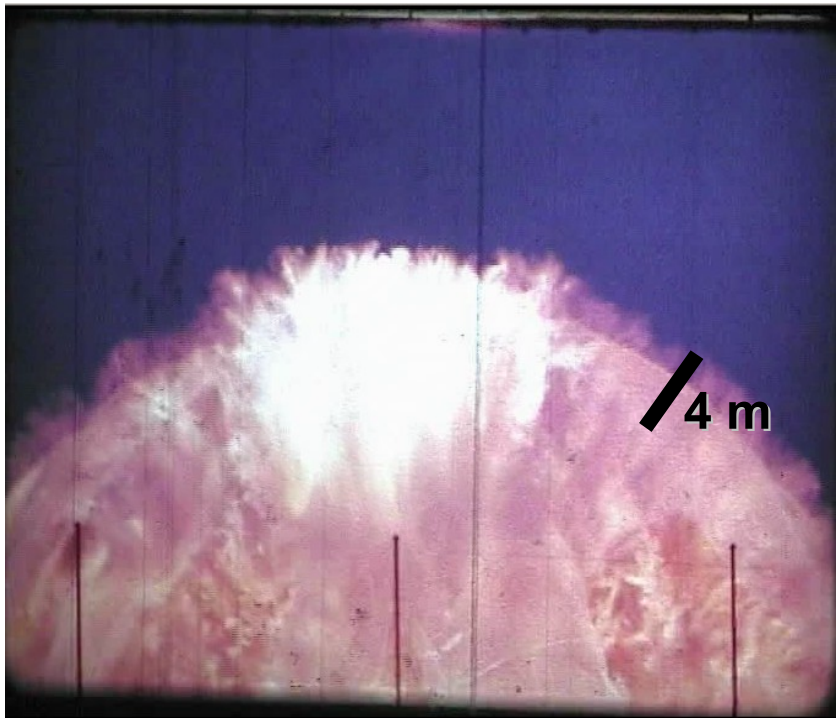

Figure 2. A snapshot of the hydrogen air flame front at a final stage of the explosion

To model a dilution of an initial hydrogen-air cloud by an atmospheric air the additional conservation equation for air mass fraction is used:

$$\frac{\partial}{\partial t}\left(\overline{\rho}\,\widetilde{Y}_a\right)+\frac{\partial}{\partial x_j}\left(\overline{\rho}\,\widetilde{u}_j\widetilde{Y}_a\right)=\frac{\partial}{\partial x_j}\left(\frac{\mu_{eff}}{Sc_{eff}}\frac{\partial \widetilde{Y}_a}{\partial x_j}\right)-\frac{\widetilde{Y}_a}{\widetilde{Y}_f+\widetilde{Y}_a}\overline{S}_c\,. \tag{3}$$

The gradient method [10] has been applied to model the source term in the progress variable equation:

$$\overline{S_c}=\rho_u S_t\left|grad\,\widetilde{c}\right|\,. \tag{4}$$

The use of the burning velocity concept and the gradient method provides a convenient way to ensure that the prescribed mass burning rate $\rho_u S_t$ takes place.

In the flamelet combustion regime the turbulence-combustion interaction is purely kinematic and chemistry enters the combustion model only through its influence on the laminar burning velocity S_u. To model an increase of the burning velocity due to the unresolved SGS effects of the hydrodynamic instability the premixed turbulent combustion model by Yakhot [11], based on RNG theory, has been adopted:

$$S_t=S_u\exp\left(\frac{u'}{S_t}\right)^2, \tag{5}$$

where S_u is the burning velocity of flamelets.

The "small-scale" turbulence generated by flame front itself changes the burning velocity of flamelets. This phenomenon can not be resolved by LES when large-scale problems are considered and has to be

modelled. To account for the corresponding flame front acceleration the burning velocity of SGS flamelets was modified:

$$S_u = S_{u0} \cdot \Xi, \tag{6}$$

where S_{u0} – laminar burning velocity for a stretched stoichiometric hydrogen-air flame, and Ξ is the flame front wrinkling due to the flame front induced turbulence. As the onset of instabilities occurs soon after the ignition, it seems that the "initial" burning velocity value reported by the authors of the experiment S_{u0}=2.39 m/s already accounts for some velocity augmentation. The value of the burning velocity of stretched stoichiometric hydrogen-air flame S_{u0}=1.91 m/s [12] was used in simulations. This value of the burning velocity was used in the range of hydrogen concentrations in diluted by air mixture down to the low flammability limit of 4% by volume as an approximation. Below the low flammability limit the source term in the progress variable equation was equal to zero.

The expansion coefficient for combustion products of stoichiometric hydrogen-air flame calculated using CHEMKIN code is E_I=7.2 and according to (1) the maximum value of the flame front wrinkling factor due to flame front induced turbulence is Ξ_{max} =3.6. According to the analysis of Gostintsev *et al*. the wrinkling factor Ξ was growing with radius of the flame front as

$$\Xi = 1 - (\Xi_{\max} - 1) \cdot \left(1 - \exp\left(R / R^*\right)\right) \tag{7}$$

with the characteristic radius of the onset of self-similar flame propagation regime R^*=1.0 m.

The solver of FLUENT software, based on the control-volume discretisation method, was used to realise the LES model. Explicit linearisation of the governing equations with explicit method for solution of linear equation set was used. Convection terms were linearised using second order accurate upwind scheme, diffusion terms – using central-difference second-order accurate scheme. The Runge-Kutta algorithm was employed for advancement of solution in time. The time step was determined from Courant-Friedrichs-Lewy condition $\Delta t = \left(CFL \cdot \Delta_{CV}\right) / \left(a + u\right)$, where the CFL number was equal to 0.8.

4.0 CALCULATION DOMAIN, INITIAL AND BOUNDARY CONDITIONS

The calculation domain had dimensions 200x200x100 m (LxWxH) to include both the flame and the pressure wave propagation areas. The tetrahedral unstructured mesh was used in the area of flame front propagation with an average control volume (CV) size from about 0.4 m close to ignition area and up to 1.0-1.2 m at $10<R\leq22$ m. Then tetrahedral CV size increased gradually with distance up to 4 m. To decrease the total number of CV, the area beyond 30 m from the ignition source was meshed using structured hexahedral grid. The average size of hexahedral CV along the direction, designated for recording pressure dynamics, was about 2.0 m and 4.0 m in the rest of the domain. The total number of CV was 309494. The calculation domain cross section and the enlargement of its area $R\leq22$ m are shown in Figure 3.

For spherical flame propagation the minimal characteristic size of the flow is large, shear stresses and, hence, turbulence generation rate, are small, and the used grid resolution was sufficient for LES. Moreover, the gradient method used for combustion model allows to decouple combustion model from grid resolution. Previous studies [8-9] show that for such flames the grid size affects simulation results through the resolution of the flame wrinkling only. Grid sensitivity analysis was conducted at preliminary stage of simulations and results are given in [13].

Non-slip adiabatic boundary conditions were applied on the ground. Non-reflecting boundary conditions were used on the boundaries in atmosphere.

Initial pressure in the calculation domain was equal p=98.9 kPa, initial temperature T=283 K. Initial value of the progress variable and the air concentration at $R \leq 10$ m were c=0, Y_a=0.9713; at R>10m: c=0, Y_a=1.0.

Ignition was modelled by an increase of the progress variable in one control volume during period t=15 ms and provided the growth of the flame front radius with time close to linear (so no adjustment of simulation results in time was required).

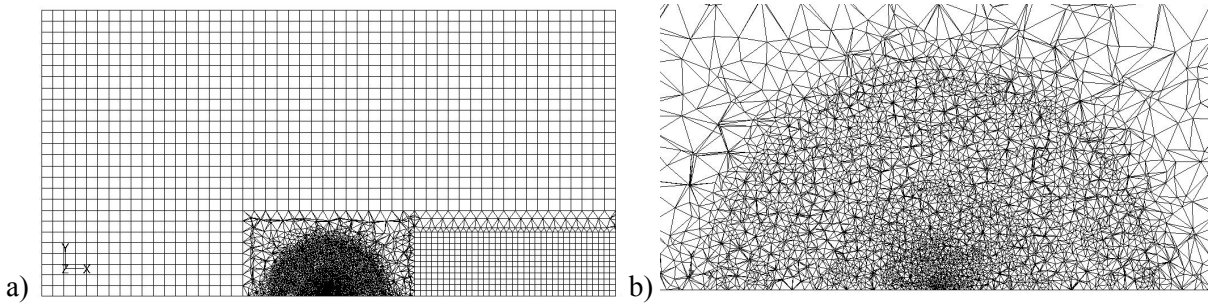

Figure 3. Cross section of the calculation domain: a) whole domain, b) enlargement of the area $R \leq 22$m

5.0 RESULTS AND DISCUSSION

The preliminary results of the present study were included into the Standard Benchmark Exercise Problem SBEP-V2 carried out in the framework of the European Network of Excellence "Safety of hydrogen as an energy carrier". The present simulation results are similar to SBEP apart from being obtained in different conditions: symmetrical calculation domain, mixed structured/unstructured grid with smoother change in control volume size, more precise procedure was used to solve SGS RNG model equation (5). These changes provided slightly different flame front propagation dynamics and significantly improved the pressure wave transients at a far field.

5.1 Flame front propagation dynamics

Figure 4 shows the simulated flame front profiles compared to experimental data. It is seen that the flame front shape is generally hemispherical and wrinkled both in experiment and simulation. The flame front is reproduced naturally on the unstructured tetrahedral mesh and no arrangements were made to keep it spherical or smooth. The model was capable to reproduce the evolving flame wrinkling in our previous studies, e.g. [9], and one can see that the flame surface is covered by the developing wrinkling structure in the present simulation as well. However, the maximum resolved flame wrinkling factor reached $\Xi_{resolved}$=1.1 in [8] and the same value can be expected in this study.

Simulated flame front propagation dynamics was found by averaging locations of the progress variable in the range $0.2 \leq c \leq 0.8$ and is shown in Figure 5. The simulated flame front propagation is in a very good agreement with the experimental data with taking into account the fact that all initial data for simulations according to the applied LES model were adopted from the literature.

Comparison of the experimental and simulated burning velocity is given in Figure 6. The burning velocity was obtained by post processing data in Figure 5: the derivative of the average flame front radius over time was divided by expansion factor E_i=7.2 to give average burning velocity of the mixture. An oscillation of burning velocity is observed at flame front radius R=10 m, which is a result of the application of our procedure of the flame front location calculation to non-uniform numerical mesh at the interface between initial hydrogen-air cloud and atmosphere. The simulated burning velocity is of the same order of magnitude as experimental one. The experimental burning velocity is growing with time and reaches, according our estimation, value S_t=13 m/s. The simulated burning velocity is accelerating up to t=0.05 s (flame radius about R=2.0 m) and then remains rather constant

and equal S_t=9.0-9.5 m/s during the most of the combustion period. It is not clear which of the following two phenomena contributed more significant to the experimental fact of monotonical increase of experimental flame propagation velocity: the fractal nature of large scale flame front surface or the "outflow" through the segments of a polyethylene balloon induced by balloon's rupture?

The flame acceleration in simulations is due to the monotonic growth of the flame wrinkling factor Ξ to its maximum value of 3.6 during the period of time when turbulence generated by flame itself develops and reaches its maximum at characteristic size of the cloud of 1 m. Averaged through the flame front the ratio of S_t / S_u , which is the modelled burning velocity augmentation due to the SGS premixed turbulent combustion, eq. (5), is of the order of 1.20 and shown in the Table 1. The modelled increase of the turbulent burning velocity is almost constant in course of the explosion and a bit higher compared to the resolved flame front wrinkling of the order of $\Xi_{resolved}$=1.10. It is clear that both resolved and modelled effects of the hydrodynamic instabilities cannot provide comparable with experiment flame acceleration alone. The main contribution to the flame front propagation velocity increase is due to the turbulence generated by flame front itself and is equal to 3.6.

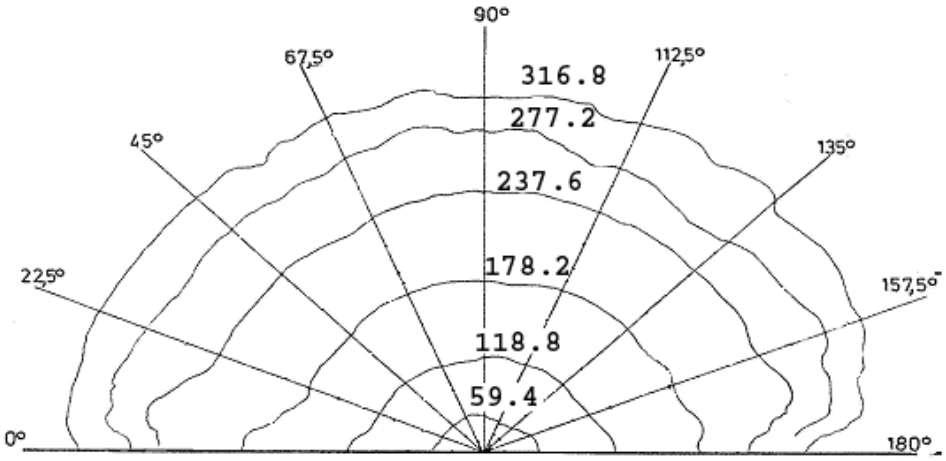

a)

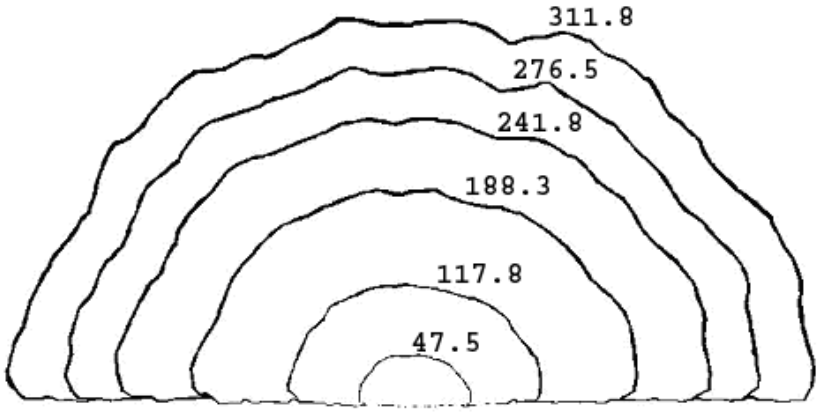

b)

Figure 4. Comparison between experimental (a) and simulated (b) flame front profiles. Numbers - time in ms

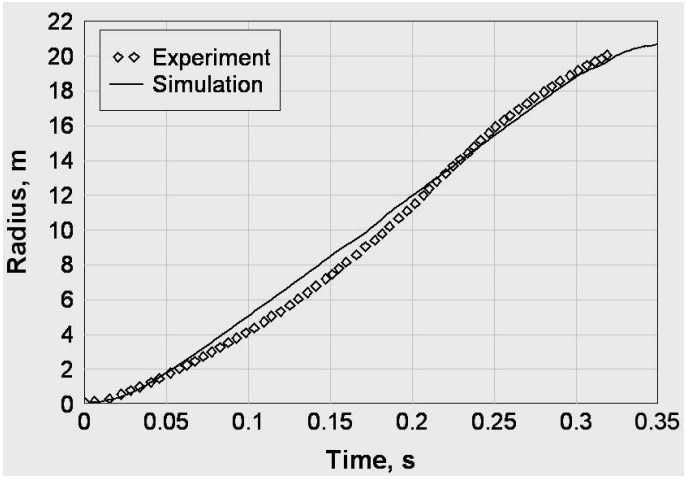

Figure 5. Comparison of the experimental and simulated average flame front radius

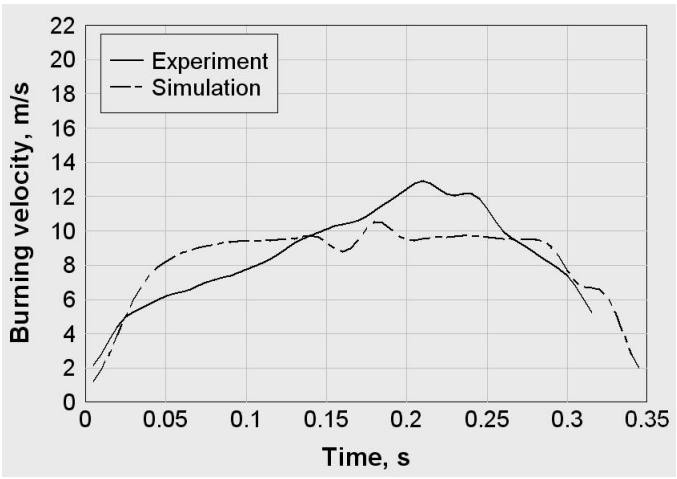

Figure 6. Comparison of the experimental and simulated burning velocity

Table 1. The SGS flame front wrinkling factor S_t/S_u (the premixed turbulent combustion model)

Time, ms	Average flame radius, m	S_t/S_u
47.4	1.66	1.25
117.8	6.31	1.22
188.3	11.18	1.21
241.2	14.85	1.18
276.5	17.24	1.21
311.8	19.31	1.23

5.2 Pressure wave dynamics

The simulated flame front propagation dynamics is shown to be in a good agreement with the experiment. Hence, a reasonable agreement between experimental and simulated pressure dynamics can be expected. Figure 7 demonstrates the comparison of the experimental and simulated pressure

dynamics at different distances from the explosion centre: 2, 5, 8, 18, 35, and 80 m. It is seen that simulated pressure wave dynamics is close to reliable experimental pressure records.

In agreement with the experimental report [7] the maximum simulated overpressure is about 6 kPa and practically constant for pressure sensors installed in the area of flame front propagation. Some deviation of the simulated pressure from the experimental one for the pressure sensor at 2 m may be explained by the fact that the sensor was affected by the combustion and its readings are not reliable after the flame front passes the location of the sensor. This is the case at least for sensors installed at 2, 8 and 18 m from the centre of the explosion: the pressure readings don't return to zero after the negative pressure wave. For the pressure sensors located outside of the area of the flame front propagation the simulated pressure dynamics (both positive and negative phases of the pressure wave) and its decay with the distance are in a good agreement with the experimental measurements.

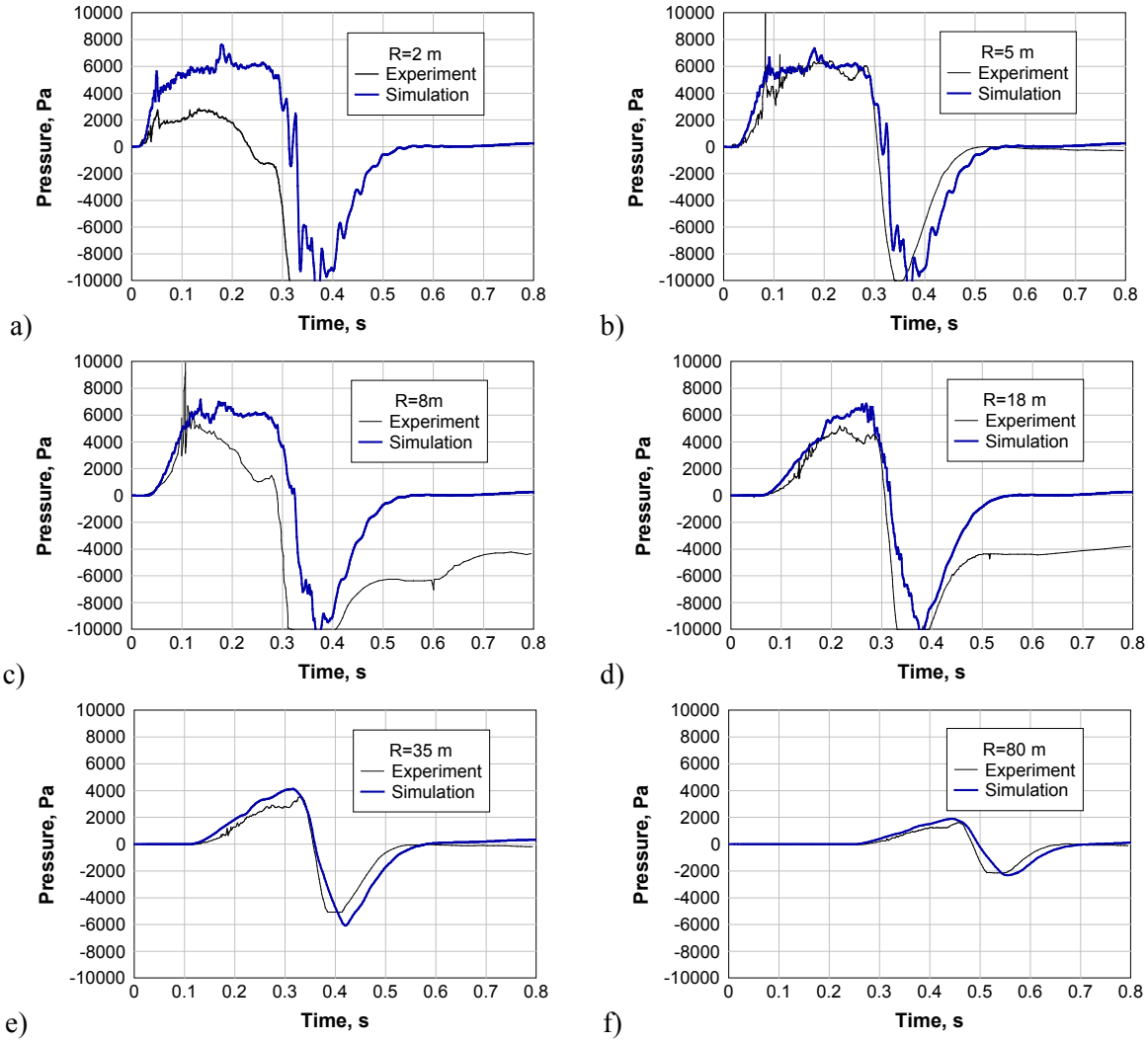

Figure 7. Comparison between experimental and simulated explosion pressure wave dynamics at different distances from the explosion centre: a) 2 m, b) 5 m, c) 8 m, d) 18 m, e) 35 m, f) 80 m

CONCLUSIONS

The LES model developed at the University of Ulster has been applied to study the dynamics of the largest unconfined deflagration of stoichiometric hydrogen-air mixture performed previously in

Germany. The model has no adjustable parameters and reasonably reproduced the experimental data on dynamics of flame and pressure wave propagation.

Effects of the hydrodynamic flow instabilities and the turbulence induced by turbulent flame front itself on the burning velocity acceleration are accounted separately in the model. It is demonstrated that the main contributor to the turbulent flame front propagation velocity is the turbulence generated by flame front itself.

Further studies have to model under resolved fractal structure of large-scale flames to reproduce in more detail the monotonous acceleration of the flame front observed in the experiment.

REFERENCES

1. Bradley, D., Possible Chronology of a Worst Case Gaseous Explosion, Paper presented at the 2nd International Conference Fire Bridge 2005, Belfast, May 2005.
2. Bradley, D., Instabilities and Flame Speeds in Large-Scale Premixed Gaseous Explosions, *Philosophical Transactions*, Royal Society of London, **A**, 1999, pp.3567-3581.
3. Groff, E.G., The cellular nature of confined spherical propane-air flames, *Combustion and Flame*, **48**, 1982, pp.51-62.
4. Karlovits, B., Denniston, D.W.Jr. and Wells, F.E., Investigation of Turbulent Flames, *Journal of Chemical Physics*, **19**, May 1951, pp.541-547.
5. Gostintsev, Yu.A., Istratov, A.G. and Shulenin, Yu.V., Self-Similar Propagation of a Free Turbulent Flame in Mixed Gas Mixtures, *Fizika Goreniya i Vzryva* (*Combustion, Explosion and Shock Waves*), **24**, No.5, 1988, pp. 63-70.
6. Bull, D.C., Critical Review of Post Piper-Alpha Developments in Explosion Science for the Offshore Industry, *Research Report 89 prepared for Health and Safety Executive, Firebrand International Ltd*, ISBN 07176 28132, 2004.
7. Schneider, H. and Pförtner, H., PNP-Sichcrheitssofortprogramm, Prozebgasfreisetzung-Explosion in der Gasfabrik und Auswirkungen von Druckwellen auf das Containment. Dezember 1983, Fraunhofer-ICT internal report.
8. Molkov, V., Makarov, D. and Grigorash, A., Cellular Structure of Explosion Flames: Modelling and Large Eddy Simulation, *Combustion Science and Technology*, **176**, Issue 5-6, pp.851-885, 2004.
9. Makarov, D. and Molkov, V., Large Eddy Simulation of Gaseous Explosion Dynamics in an Unvented Vessel, *Combustion, Explosion and Shock Waves*, **40**, No.2, 2004.
10. Laskey, K.J., Oran, E.S. and Boris, J.P., The Gradient Method for Interface Tracking, Naval Research Laboratory Memorandum Report 6183, 1988.
11. Yakhot, V., Propagation Velocity of Premixed Turbulent Flames. *Combustion Science and Technology*, **60**, 1988, pp.191-214.
12. Lamoureux, N., Djebaili-Chaumeix, N. and Paillard, C.E., Laminar Flame Velocity Determination for H_2-Air-Steam Mixtures using the Spherical Bomb Method, *Journal de Physique IV*, **12**:Pr7, 2002, pp.445-452.
13. Gallego, E., Migoya, E., Martín-Valdepeñas, J.M. et al., An Intercomparison Exercise on the Capabilities of CFD Models to Predict Distribution and Mixing of H_2 in a Closed Vessel, Proceedings of 1st Int. Conference on Hydrogen Safety, Pisa, 8-10 September 2005 (accepted for presentation).